Double-pillared cobalt Pacman complexes

Post-print of a peer-reviewed article published by the Royal Society of Chemistry.
Published article available at: http://dx.doi.org/10.1039/C1DT11424G

Cite as:
Devoille, A. M. J., & Love, J. B. (2012). Double-pillared cobalt Pacman complexes: synthesis, structures and oxygen reduction catalysis. *Dalton Transactions*, 41(1), 65-72.

Manuscript received: 27/07/2011; Accepted: 09/09/2011; Article published: 26/10/2011

Double-pillared cobalt Pacman complexes: synthesis, structures and oxygen reduction catalysis**

Aline M. J. Devoille[1] and Jason B. Love[1,*]

[1]EaStCHEM, School of Chemistry, Joseph Black Building, University of Edinburgh, West Mains Road, Edinburgh, EH9 3JJ, UK.

[*]Corresponding author; e-mail: jason.love@ed.ac.uk, fax: +44 131 6504743, tel: +44 131 6504762

[**]We thank EaStCHEM and the University of Edinburgh for support and Prof. A. M. Z. Slawin (University of St. Andrews) and Dr. F. J. White (University of Edinburgh) for their assistance with some of the crystallographic characterisation.

Supporting information:
† Electronic supplementary information (ESI) available: Fig. S1–S5, Tables S1–2. CCDC reference numbers 815017–815019. For ESI and crystallographic data in CIF or other electronic format see http://dx.doi.org/10.1039/C1DT11424G

Graphical abstract:

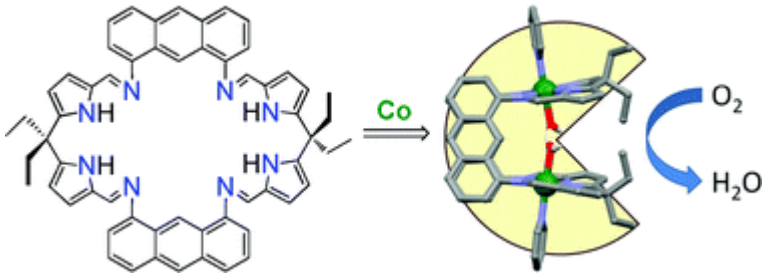

Keywords:
porphyrin-corrole dyads; electrocatalytic 4-electron reduction; dicobalt cofacial porphyrin; schiff-base calixpyrroles; coupled electron-transfer; o bond activation; fuel-cells; binucleating ligands; hangman porphyrins; oxidation-state

Abstract

The syntheses and structures of binuclear cobalt complexes of a double-pillared cofacial Schiff-base pyrrole macrocycle (L) were determined and their activity as catalysts for the oxygen reduction reaction evaluated. The new binuclear cobalt complex, $[Co_2(L)]$, **1** was formed in good yield using a salt-elimination method and was characterised as adopting a cofacial structure in solution by NMR spectroscopy and as its THF and pyridine solvates in the solid state by X-ray crystallography. Using a variety of spectroscopic techniques, this complex was found to react reversibly with dioxygen to form a new paramagnetic complex. Furthermore, the new aqua-hydroxy double salt $[Co_2(\mu\text{-}H_3O_2)(py)_2(L)][BF_4]$ **2** was characterised by X-ray crystallography. In acidified benzonitrile solution, **1** behaves as a catalyst for the selective four-electron reduction of dioxygen to water and showed a large improvement in efficacy compared to its *o*-phenylene Schiff-base analogues.

Introduction

The four-electron reduction of oxygen to water is a reaction that is intrinsic to fuel cell technology,[1] and is commonly catalyzed at the cathode by platinum impregnated in carbon.[2] However, the high loadings of this precious metal that are required to achieve appreciable activity, combined with issues of decomposition and deactivation through poisoning has led to a plethora of research into new catalysts derived from base metals such as Co and Fe.[3, 4] Significantly, it has been found recently that combinations of Co and polypyrrole,[5] or pyrolyzed Fe or Co nitrogen-doped carbonaceous materials[6, 7] exhibit activities and longevity that approach those of Pt-based electrodes. Even with these elegant advances, the study of molecular compounds that can catalyze oxygen reduction remains important as it can provide synthetic, structural, and mechanistic information not available for more complex, and generally surface-based systems.

Binuclear cofacial diporphyrins and dicorroles, especially those of cobalt, have been intensively studied as they can act as catalysts for the four-electron reduction of oxygen. Important mechanistic details of the oxygen reduction reaction (ORR) have been elucidated through evaluation of these molecular systems, such as the significance of the M···M separation, the acid-base characteristics of the system, and the proposed key involvement of the superoxo-intermediate as a director of reaction selectivity.[8-12] Furthermore, the second metal, which can facilitate binuclear O_2 binding and adjust the pKa of dioxygen adducts so favouring four-electron chemistry, can also be replaced by a suitable hydrogen bond donor or acid/base appendage.[13]

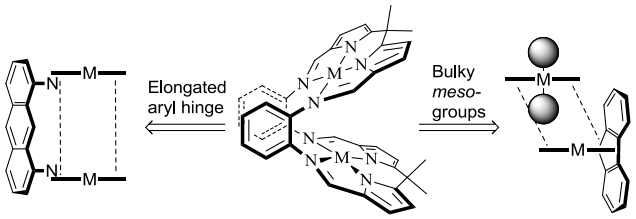

Chart 1. The effects of ligand design on the Schiff-base pyrrole macrocycle H_4L^o and its bimetallic complexes.

As alternatives to cofacial diporphyrins that are typically difficult and time-consuming to synthesize, we have developed straightforward synthetic procedures to Schiff-base pyrrole macrocycles which, on metallation, form similar 'Pacman-shaped' bimetallic structures in which the primary metal coordination sphere and separation are well-controlled.[14] These macrocycles were also developed independently by Sessler and co-workers.[15] Binuclear cobalt complexes of the first generation macrocycle H_4L^o (Chart 1) were isolated and the peroxo complex $[Co_2(\mu\text{-}O_2)(py)_2(L^o)]$ characterised structurally; the peroxo ligand was found to bridge the two metals within the molecular cleft in a Pauling bonding mode.[16] This preference for the formation of the peroxo complex, combined with the tendency to form stable hydroxo-bridged compounds, led to poor activity in oxygen reduction catalysis.[17] Modification of the *meso*-substituent from methyl to fluorenyl (H_4L^f) was used as a strategy to minimize the formation of single-atom-bridged complexes (Chart 1 right), and promoted the preferential formation of the superoxo cation $[Co_2(\mu\text{-}O_2)(py)_2(L^f)]^+$ which was characterised structurally.[18] Furthermore, this complex was found to act as a catalyst for oxygen reduction, albeit less effectively than the cofacial diporphyrin analogues. As a second modification, we have developed a new macrocyclic ligand (H_4L, Chart 1 left, and Scheme 1) in which the two Schiff-base-pyrrole N_4-donor compartments are separated by two anthracene pillars.[19] This ligand modification resulted in a double-pillared, cofacial arrangement of the PdN_4 compartments in $[Pd_2(L)]$ that is similar to the structures seen in complexes of single-pillared cofacial diporphyrins. We describe here the synthesis and structures of new binuclear cobalt complexes of L, evaluate their application as catalysts for the oxygen reduction reaction (ORR), and provide a comparison of the catalytic activity to the earlier generation cobalt macrocyclic Pacman complexes.

Results and Discussion

Synthesis and structures of Co(II) complexes of L

The in-situ synthesis of the lithium salt $[Li_4(L)]$ in THF followed by reaction with cobalt chloride generated the binuclear cobalt complex $[Co_2(L)]$, **1** as a red precipitate in 51% isolated yield (Scheme 1).

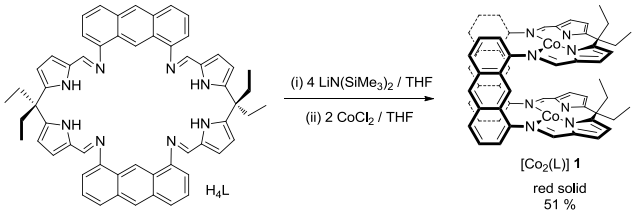

Scheme 1. Synthetic route to the new Schiff-base Pacman macrocyclic complex [Co_2(L)], **1**.

The ^{1}H NMR spectrum of **1** in THF/C_6D_6 displays 11 resonances between 40 and −60 ppm, one resonance short of the 12 expected for a paramagnetic complex of cofacial structure in which the ethyl groups adopt *endo*- and *exo*-positions relative to the bimetallic cleft. However, the presence of two resonances at -17.1 and -18.2 ppm for 6H each confirms that **1** adopts a cleft structure in solution. The formation of **1** is further supported by the absence of a NH vibration in the IR spectrum and ν(C=N) at 1580cm^{-1}, similar to that seen for [Pd_2(L)] (ν(C=N) 1570 cm^{-1}).[19] Crystals of [Co_2(L)][Co_2(*exo*-THF)$_2$(L)]·3PhMe (**1** and **1.THF**), in which both unsolvated and THF-solvated components were present in the asymmetric unit were grown from a THF/toluene mixture while crystals of the pyridine adduct [Co_2(*exo*-py)$_2$(L)]·4THF, **1.py** were grown from a mixture of pyridine, THF, and hexane. The solid state structures of both sets of crystals were determined and are shown in Figure 1, with crystal data and selected bond lengths and angles detailed in the Supplementary Information, Tables S1 and S2, respectively.

In the unsolvated complex **1**, the double-pillared anthracenyl backbone is face-to-face π-stacked with a shortest C-C separation between opposing aryl rings of 3.368(7) Å and deviation from co-planarity of 9.8°. The two N_4-donor planes form a bite angle of 18.1° and display a mean twist angle of 28.8°. The two pseudo-square planar cobalt cations are located 0.05 Å from their respective N_4-donor planes towards the intramolecular cavity leading to a Co3···Co4 separation of 5.471(2) Å. In the solvated complexes, **1.THF** and **1.py**, the two N_4-donor planes deviate from co-planarity by 19.8° and 16.2° for THF and pyridine-solvated complexes, respectively, and the mean C_2-twist angle between the metal-coordination plane and the anthracenyl backbone is 30.7° and 28.6°. The two cobalt cations are separated by 5.710(2) and 5.8139(2) Å in pseudo-square pyramidal environments with the metal centers in the basal plane and the oxygen of the THF molecule or the nitrogen of the pyridine molecule in the apical site. All solvent molecules are located in sites exogenous to the molecular cavity which suggests that endogenous solvent coordination is inhibited. The geometric parameters of these new cobalt complexes are very similar to those seen for the cofacial diporphyrin complex [Co_2(DPA)] in which the two porphyrin compartments are separated by a single anthracene pillar (Table 1). It is likely that the difference seen in the bite angle between the two N_4-donor compartments (ca. 18^o vs. 3^o) is due to the extra steric interactions that occur between the ethyl *meso*-substituents in the [Co_2(L)] complexes.

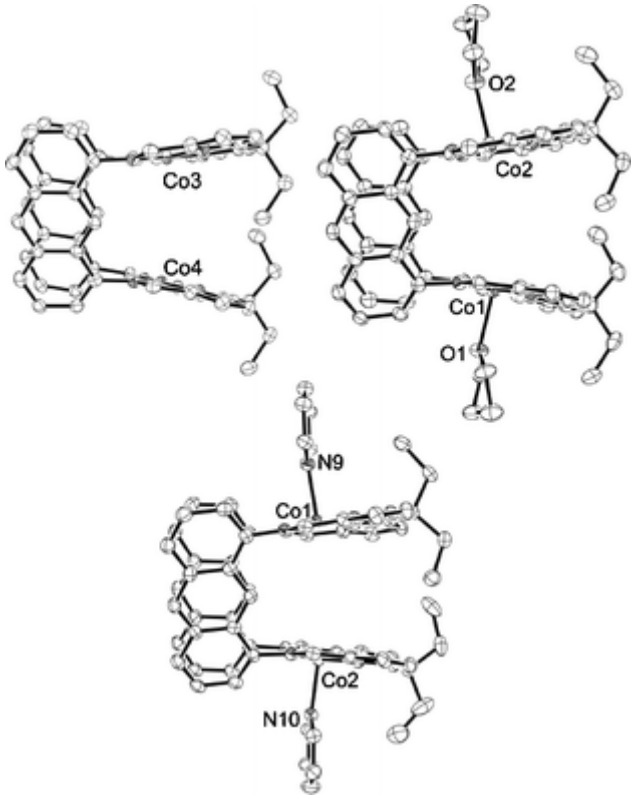

Figure 1. Solid state structures of **1** showing unsolvated **1** (top left) and THF-solvated **1.THF** (top right) from the asymmetric unit and pyridine-solvated **1.py** (bottom). For clarity, all hydrogen atoms and solvent of crystallization are omitted (50% probability displacement ellipsoids, relative positions of **1** and **1.THF** arbitrary).

Table 1. Structural parameters for dicobalt complexes of macrocycle L

	1	**1.THF**	**1.py**	**2**	**Co_2(DPA)[a]**
Co··Co (Å)	5.47	5.71	5.84	5.57	5.53
Co o.o.p (Å)[b]	+0.05	-0.08	-0.18	-0.06	+0.03
Twist (°)[c]	28.8	30.7	28.6	24.3	36.6
Bite (°)[d]	18.1	19.8	16.2	18.5	3.0
An··An (°)[e]	9.8	14.3	11.8	7.0	n/a
C_{an}··C_{an} (Å)[f]	3.37	3.51	3.21	3.44	n/a

[a] ref [20], DPA = anthracene-pillared diporphyrin; [b] distance of Co out-of-N_4 plane, +ve value describes translation into cleft; [c] mean dihedral angle between anthracene and N_4-donor planes; [d] dihedral angle between opposing N_4-donor planes; [e] dihedral angle between opposing anthracene pillars; [f] shortest intramolecular anthracene C-C separation

Reactions of 1 with O_2

We have shown previously that binuclear cobalt complexes of macrocyclic Pacman ligands derived from 1,2-substituted diaminobenzenes spontaneously and irreversibly bind dioxygen in THF and, in presence of pyridine, can be isolated and characterised crystallographically as either peroxo or superoxo complexes.[16-18] In contrast, **1** does not react with oxygen in THF or even in neat pyridine. This behaviour is more comparable to that seen for binuclear Co^{II} cofacial diporphyrin complexes, which, in the absence of a bulky axial base such as a dialkylated imidazole, do not bind dioxygen.[12, 21, 22] However, it was found that exposure of **1** to dioxygen in PhCN caused the red solution to turn dark brown, an indication of a reaction. This reaction was monitored by ^{1}H NMR spectroscopy, EPR spectroscopy, UV-visible spectroscopy, and cyclic voltammetry and was found to be reversible.

On exposure to O_2, the paramagnetic ^{1}H NMR spectrum of **1** in PhCN is replaced by a series of very weak resonances between 25 and −20 ppm that are indicative of the formation of a small quantity of a new paramagnetic material (Supporting Information, Figure S1). Significantly, no resonances consistent with a diamagnetic $Co^{III}Co^{III}$ peroxo complex are seen (Equation 1), and cycling the sample back under N_2 results in the re-appearance of the NMR spectrum of **1** combined with the disappearance of the weak paramagnetic resonances. It is clear that on exposure to O_2, the major product is paramagnetic and NMR silent.

The X-band EPR spectra of **1** in fluid PhCN solution under either N_2 or O_2 were silent, as was the EPR spectrum in frozen solution under N_2 (Supporting Information, Figure S2). However, the frozen solution spectrum under O_2 displays a broad, featureless signal at *g* 2.07 which is lost by cycling the sample back under N_2. Unfortunately, the lack of hyperfine makes characterization of this species difficult, although these data preclude the formation of the superoxo cation $[Co^{III}Co^{III}(O_2)(L)][OH]$ (Equation 2) as the related cobalt cofacial diporphyrin complexes show the expected 15-line EPR spectra in both fluid and frozen solution.[11, 23, 24] In the presence of a strong axial base such as N-methylimidazole, these latter porphyrinic complexes form rapidly and irreversibly on oxygenation of the $Co^{II}Co^{III}$ precursors due to stabilisation of the Co^{III} oxidation state.[22, 23] In our case, it is likely that PhCN,[25] unlike THF and pyridine, acts as an axial donor that facilitates a degree of O_2 binding to form the adduct $[Co^{II}Co^{II}(O_2)(L)]$ **1-O_2** (Equation 3). The binding of O_2 to **1** may arise due to a spin state change that appears to only occur in PhCN solution. The effective moment μ_{eff} of **1** is seen to decrease from 3.55 μ_B in THF to 1.69 μ_B in PhCN, which, on binding of O_2, increases slightly to 1.97 μ_B. In conjunction, the linearity of PhCN compared to THF and pyridine may limit its ability to coordinate within the bimetallic cleft, so allowing an interaction with O_2. As facile and reversible electron transfer reactions have been seen previously in cofacial diporphyrin chemistry,[23] internal electron-transfer and subsequent formation of the neutral, mixed-valence superoxo complex $[Co^{II}Co^{III}(O_2^{-})(L)]$. However, more detailed EPR data are required to be able to characterise this complex.

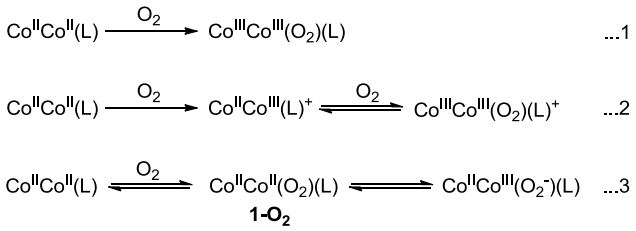

The UV-visible spectrum of **1** under nitrogen consists of a broad absorption at 430 nm (ln ε = 10.7) and a shoulder at 355 nm (ln ε = 11.0) (Supplementary Information, Figure S3). Upon degassing the sample and exposure to dioxygen, these absorptions are replaced by bands at 449 nm (ln ε = 10.8) and 358 nm (ln ε = 11.4); these spectrophotometric changes are similar to those exhibited by the porphyrinic analogues [Co_2(DPA)] and [Co_2(DPB)].[25] As in the above experiments, return to the original UV-visible spectrum was observed when the sample was placed back under an inert atmosphere, confirming the reversibility of the dioxygen binding.

The CV of **1** under N_2 in PhCN (Bu_4NBF_4, Fc^+/Fc) displays two successive and pseudo-reversible oxidations at E_p^a –0.34 and –0.20 V (Supporting Information, Figure S4); on scanning to potentials > +0.2 V, these oxidations become irreversible due to a chemical transformation that occurs at higher potentials. Analysis of the CVs of the related binuclear zinc complex [Zn_2(L)][26] show that no ligand redox activity occurs during the same potential window. As such, these two redox events are best attributed to stepwise Co^{II} to Co^{III} oxidation and suggest that electronic communication occurs between the metals. On scanning to more negative potentials, a third pseudo-reversible wave is seen at E_p^c –2.32 V. This feature is also not observed in the Zn analogue [Zn_2(L)] and so is likely to be due to reduction of Co^{II} to Co^{I}. The oxidation of **1** is similar to those of the diporphyrinic analogues. For example for [Co_2(DPX)], in which the two porphyrins are separated by a xanthene pillar, two reversible one-electron oxidations at + 0.08 and + 0.22 V (values adjusted to Fc/Fc^+ in MeCN,[27] originally *vs*. SCE in PhCN) are seen and are assigned as sequential Co^{II}/Co^{III} oxidations.[10] In contrast, for [Co_2(DPA)] in which the two porphyrins are separated by an anthracene pillar, two quasi-reversible, two-electron oxidation waves are seen at +0.00, and +0.35 V (*vs*. Fc/Fc^+ in PhCN). In this latter example, this indicates that no electronic communication occurs between the oxidizing centres even though they are separated by a similar distance.[12, 28] Extensive spectroelectrochemical analysis of [Co_2(DPA)] led to the assignment of the two-electron oxidation at +0.35 V as metal-based while that at 0.00 V was the result of concurrent oxidation of the two porphyrins. Even so, all oxidized forms of [Co_2(DPX)] and [Co_2(DPA)] were found to react with O_2 to form superoxo complexes, as evidenced by EPR spectroscopy. For **1**, exposure to O_2 results in the loss of all of these features in the CV and the appearance of a quasi-reversible reduction wave at E_p^c –1.9 V (*vs.* Fc/Fc^+) consistent with background O_2 reduction by the Pt electrode. As with the above spectroscopic data, return to a N_2 atmosphere causes the reappearance of the CV associated with **1**, and corroborates the reversibility of O_2 binding.

Structural characterization of an aqua-hydroxy double salt

We have been unable to grow crystals of the product of the reaction between **1** and O_2 and so cannot confirm its identity. However, when a dilute (mM) solution of **1** in an electrolyte mixture of PhCN, Bu_4NBF_4 and pyridine was exposed to air, a small number of crystals were formed and were found to be the new binuclear $Co^{III}Co^{III}$ complex $[Co_2(\mu\text{-}H_3O_2)(exo\text{-}py)_2(L)][BF_4]$ **2** (Figure 2, Table 1 for characteristic geometric data, and Supporting Information, Tables S1 and S2 for crystal data and selected bond lengths and angles, respectively); due to the lack of material isolated, no further characterisation of **2** was made.

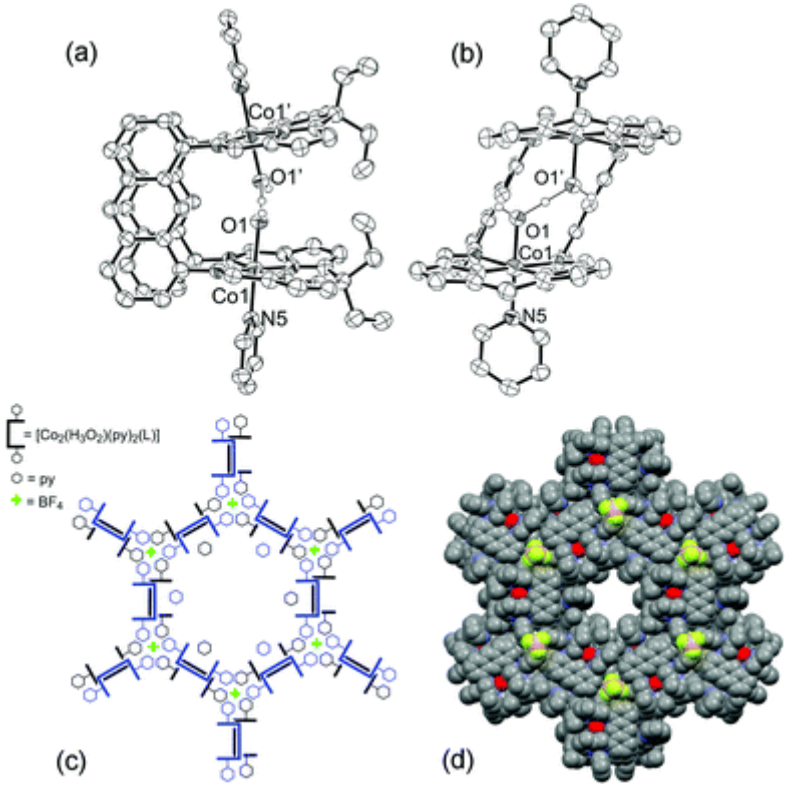

Figure 2. X-ray crystal structure of $[Co_2(\mu\text{-}H_3O_2)(py)_2(L)][BF_4]\cdot 1.8py$ **2**: (a) side-on; (b) face-on; (c) depiction of molecular packing; (d) space-fill representation of the packing, view along c-axis. For clarity, all hydrogen atoms except those on O1 and O1', the BF_4^- anion in the ORTEP diagrams, and solvent of crystallization are omitted (where shown, displacement ellipsoids are drawn at 50 % probability).

As with the complexes described above, **2** adopts a double-pillared Pacman structure in which the two CoN_4 donor compartments are approximately cofacial and splayed apart by 18.5°, the anthracenyl backbones are π-stack with a shortest C-C separation of 3.443(6) Å, and the molecule has a crystallographically-imposed C_2-symmetrical twist of 24.3°. The Co cation is octahedral with pyridine in the exogenous axial position and a

Co1-N5 distance of 1.973(3) Å that is consistent with a Co^{III} oxidation state.[16] The endogenous coordination sites are occupied by the aqua-hydroxy group $H_3O_2^-$ in which one hydrogen symmetrically bridges the two oxygen atoms; the hydrogen atoms of this latter unit were identified in the difference Fourier map and refined with bond distance restraints and riding thermal parameters. The Co1-O1 bond distance (1.929(2) Å) and O1···O1' separation (2.455(3) Å) are similar to those seen in other transition metal 'aqua hydroxy double salts' (TM-O 1.87-2.06 Å, mean 1.93 Å; O···O 2.41-2.52 Å, mean 2.45 Å, 22 examples).[29] Structural data for two related Co complexes $[\{Co(en)_2(X)\}_2(H_3O_2)]^{3+}$ ($X = NO_2^-$, SCN^-) have been reported and display significantly shorter Co-O (1.906(6)/1.911(5) Å) and O···O (2.412(9)/2.415(6) Å) distances, respectively;[30] the longer distances seen in **2** may be a consequence of structural imposition by the macrocyclic ligand. More recently, a dicobalt bis(aqua-hydroxy) complex of a binucleating pyridine phenolate has been characterised structurally and exhibits asymmetric Co-O bond distances but similar O···O bond separations (average 2.442 Å) to those seen in **2**.[31] In contrast to cobalt complexes of the variants of L, for which peroxo,[16] superoxo,[18] and now aqua-hydroxy species have been characterised crystallographically, structural information for related cobalt cofacial diporphyrin complexes that incorporate oxygen species is unknown.

Examination of the extended solid state structure of **2** reveals that an interesting hexagonal structural motif has formed (Figures 2c and 2d). The assembly of three molecules of **2** through axial pyridine C-H···F-BF_3 hydrogen-bonding interactions (C···F 2.84-3.00 Å)[32] results in a three-fold node from which the hexagonal structure evolves. The molecules are arranged such that the anthracenyl backbone alternates 'in-to' and 'out-of' the resulting cavity with the BF_4^- anions positioned above and below the molecular planes so providing an interlayer interaction. This results in an infinite columnar structure along the *c*-axis of approximately 12 Å diameter that is fully accessible to a spherical probe of 1.15 Å radius along its length. This void contains disordered and poorly-defined pyridine solvent of crystallization and also the remaining BF_4^- anions which could not be modelled satisfactorily and so were accounted for using the SQUEEZE routine of PLATON.

The assembly of discrete metal complexes into large, cyclic structures and metal-organic frameworks in which the metal complex retains potential catalytic function is becoming increasingly prevalent.[33] A vanadyl salen complex was found to form a hexameric wheel structure in the solid state, in which weak O=V···O=V interactions linked each monomer unit.[34] Alternatively, cyclic structures of metal complexes have also been generated by linking M(porphyrin) subunits through covalent interactions.[35] Furthermore, we reported recently how discrete Co Pacman complexes derived from a ditopic Schiff-base pyrrole/polyether macrocycle assembled into cyclic hexameric structures in the solid state through hydroxide-water-polyether hydrogen bonding interactions.[36]

Oxygen reduction catalyzed by 1

A 1.0 mM solution of **1** in aerated THF was used to drop coat a glassy carbon disk and the resulting modified

electrode assessed for catalytic oxygen reduction by rotating ring disk electrochemistry in 1.0 M CF_3CO_2H (Supporting information, Figure S5). While a reduction wave consistent with O_2 reduction was seen at an onset voltage of *ca.* + 0.25 V *vs*. AgCl/Ag, this feature diminished during repeat experiments and became absent after 3 cycles; polishing the electrode and re-coating with **1** caused the signal to re-appear. During these experiments, no current was seen at the Pt ring (normalized to 23 % efficiency) which shows that hydrogen peroxide is not formed and implies that only four-electron reduction of oxygen to water occurs. The loss of oxygen-reduction activity on repeat cycles is commonplace when using non-platinum metal compounds as catalysts, including those bound in N_4-donor sets, and has been attributed to either ligand degradation by reactive oxygen species formed during the catalytic cycle or release of the labile metal into solution.[4] Methods such as high-temperature annealing have been employed to access modified electrodes that are more stable to oxidative stress and in some cases have been particularly successful, generating electrodes that proffer good activity over long time periods.[7] However, thermal degradation of the well-defined complex makes analysis of the structure of the resulting catalytic species and the mechanism of reaction extremely difficult.

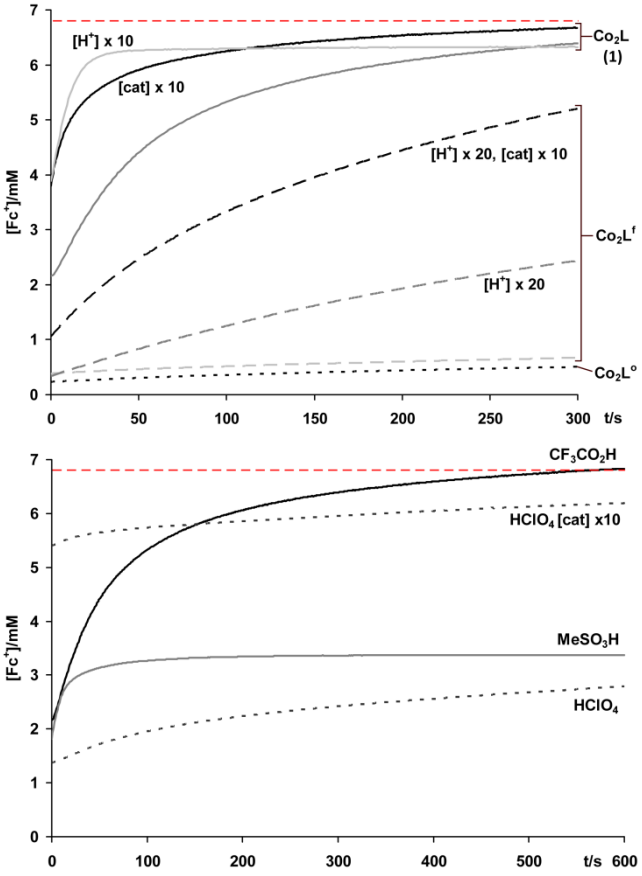

Figure 3. Production of Fc^+ at 620 nm (ε =330 $M^{-1}cm^{-1}$) in the reduction of oxygen by Fc in acidic PhCN solution catalyzed by binuclear cobalt Pacman complexes monitored by UV-Vis spectrophotometry ([H^+] =

[CF_3CO_2H]). Top: Comparison between [$Co_2(L^o)$], [$Co_2(L^f)$], and **1** at various concentrations of catalyst with CF_3CO_2H (standard conditions [O_2] 1.7 mM, [CF_3CO_2H] 0.02 M, [Fc] 0.1 M, [**1**] 0.02 mM); bottom: variation of acid using **1** as the catalyst (pKa in CH_3CN: CF_3CO_2H 12; $MeSO_3H$ 8; $HClO_4$ 2);[37] dotted red line represents the concentration of Fc^+ (6.8 mM) necessary for complete four-electron reduction.

In order to gain a better understanding of the role of **1** in the ORR, in particular to probe the selectivity of the four-electron reduction over the two-electron chemistry, oxygen reduction reactions were monitored by UV-visible spectrophotometry in acidified PhCN solution using ferrocene (Fc) as the electron source (Figure 3). To enable some correlation to the ORR catalyzed by binuclear cobalt cofacial diporphyins, the conditions used were similar to those employed by Fukuzumi and Guilard,[10] except that the weaker acid CF_3CO_2H (pKa in MeCN = 12) was used instead of $HClO_4$ (pKa in MeCN = 2).[37] Under these former conditions, no background reaction is seen in the absence of catalyst, unlike that observed when using the stronger acids and which can impact on the monitoring of the reaction if the catalyzed rate is slow. The addition and rapid mixing of a solution of CF_3CO_2H in PhCN to a mixture of Fc, **1**, and O_2 in PhCN with O_2 as the limiting reagent (1.7 mM) caused the production of ferrocenium (Fc^+), observed in the UV-visible spectrum. The reaction was found to be rapid, becoming asymptotic after *ca*. 300 s, and the average quantity of Fc^+ produced during this reaction over four separate experiments, 5.78 mM, equates to 85% conversion or the transfer of 3.4 electrons per molecule of O_2 (Figure 3 top, best result shown). With a higher concentration of acid ([**1**] 0.02 mM, [Fc] 0.1 M, [O_2] 1.7 mM, [CF_3CO_2H] 0.2 M) the production of Fc^+ was found to become asymptotic within seconds. Iodometric titrations of the mixtures at the end of the reaction showed that no hydrogen peroxide is formed, corroborating that determined above by RRDE and showing that the four-electron reduction mechanism is prevalent. Attempts to elucidate the fine detail of the mechanism of this reaction through kinetic analysis were thwarted by the rapidity of the reaction at low concentrations of Fc and future experiments would require the use of stopped-flow techniques.

Comparison can be made between reactions catalyzed by the double-anthracenyl-pillared complex **1** and its double-pillared *o*-disubstituted benzene analogues [$Co_2(L^o)$] and [$Co_2(L^f)$] which have methyl and fluorenyl-substituents in the *meso*-positions, respectively. It is clear that the efficacy of **1** in the ORR is significantly improved when compared to the other examples under all conditions. While [$Co_2(L^f)$] was shown to catalyze selectively the four-electron reduction reaction, with no hydrogen peroxide seen by iodometric titration, complete conversion was observed only when higher concentrations of catalyst and acid were used which suggested that the catalyst had limited turnover.[18] Furthermore, longer reaction times were required for the reaction to go to completion, although the use of the more reducing $Fe(C_5H_4Me)_2$ accelerated the rate of reaction. In contrast, for **1**, higher concentrations of either catalyst or acid lead to the completion of the reaction within *ca*. 100s.

It is also interesting to note that for **1** the four-electron reduction reaction proceeds using CF_3CO_2H (pKa 12) as the source of acid and that the use of stronger acids such as $MeSO_3H$ (pKa 8) or $HClO_4$ (pKa 2) results in incomplete conversion (Figure 3, bottom). These results contrast to those seen in cofacial diporphyrin chemistry in that ORR catalyzed by these latter complexes requires stronger acids such as $HClO_4$ for solely four-electron chemistry to occur,[9] as the use of acids with pKa > 12 resulted in a significant drop in selectivity. Using these latter data, it was reasoned that the basicity of the superoxide intermediate was a key director of the catalytic cycle, i.e. protonation of a basic superoxo ligand resulted in O-O bond scission, whereas rapid initial electron transfer generated peroxide preferentially. Using this rationale as a basis for **1**, it is therefore likely that the transiently-formed oxygenated species **1-O_2** contains an oxygen ligand which is rapidly protonated, so favouring O-O bond scission in preference to electron-transfer and the ultimate formation of peroxide. The behaviour of this complex under more strongly acidic conditions is less-easily rationalized, but it is clear that the use of higher concentrations of catalyst promotes complete conversion of O_2, which is the limiting reagent (Figure 3). This suggests that competition occurs between oxygen-reduction catalysis and catalyst decomposition, the latter possibly occurring through the substitution of Co^{2+} by 2 H^+ by the stronger acid, i.e. the labile metal is stripped from the ligand.

It is apparent from our previous work that the effectiveness of earlier generations of these macrocyclic Pacman complexes in the ORR relates to disfavouring the formation of peroxide or hydroxy-bridged complexes, features that are consistent with the porphyrinic analogues. For $[Co_2(L^o)]$, there is a 90:10 preference for the formation of the crystallographically-characterised peroxo complex over the superoxide, with no interconversion seen between these two species.[16, 17] This preference for the peroxide results in an ever-diminishing quantity of superoxo cation during the catalytic reaction and hence, even though no H_2O_2 is formed, this complex is not effective as a catalyst.

For $[Co_2(L^f)]$, the fluorenyl substituents affect the chemistry such that no peroxide complex is seen on exposure to oxygen. In this case, only the superoxide complex $[Co^{III}_2(O_2)(py)_2(L^f)][OH]$ and the mixed-valence complex $[Co^{III}Co^{II}(OH)(py)(L)]$, related to the superoxide complex by oxygen loss, are formed.[18] EPR measurements quantified the superoxo complex as *ca*. 25% of the mixture and it is likely that it is this higher concentration of superoxo complex that makes $[Co_2(L^f)]$ a more effective ORR catalyst. However, the preference for the formation of the bridged hydroxide complex over the superoxide complex clearly affects the ORR catalysis, so necessitating higher concentrations of catalyst and acid to enable the four-electron reduction reaction to go to completion.

In contrast to these *o*-phenylene-backboned macrocyclic complexes, the separation of the two Co centres through the use of the double-anthracenyl pillars in **1** appears to inhibit the spontaneous formation of undesired oxygenates. Furthermore, solutions of **1** in THF or pyridine are inert to oxidation. However, in PhCN the reversible formation of a new paramagnetic compound is seen, and is reflected in this compound's capacity to act as an efficient catalyst for the ORR. The stoichiometric and catalytic behaviour of this

compound is similar to that shown by the related cofacial diporphyrin complex [Co_2(DPA)] in which the two porphyrinic compartments are separated similarly by an anthracenyl spacer.[25] However, catalysis by **1** proceeds using an acid with a much lower pKa, indicating that the basicity of the coordinated oxygen ligand is higher.[9] Furthermore, the aqua-hydroxy complex **2**, isolated from an air-exposed pyridine solution of **1** in the presence of BF_4^-, is a possible intermediate in the overall catalytic cycle.

Conclusions

We have shown that modular variations of structure-directing features of straightforwardly-synthesized Schiff-base pyrrole macrocycles result in considerable changes to the chemistry of cobalt Pacman complexes of this ligand class. By elongating the spacers between the two N_4-donor compartments from *o*-phenylene to anthracene, new binuclear cobalt complexes that adopt cofacial structures are formed. Significantly, these new complexes act as efficient and selective catalysts in PhCN solution for the four-electron reduction of oxygen to water, displaying activity similar to that of the well-known cofacial diporphyrin analogues. The straightforward synthesis of these macrocyclic ligands and their complexes from inexpensive starting materials, combined with the ability to modify the catalytic activity through simple and modular ligand variation, makes these compounds promising candidates for a variety of catalytic electroreduction reactions.

Experimental Section

The synthesis of H_4L was carried out as described in the literature;[19] all other chemicals were used as purchased. Except where stated, synthetic procedures were carried out under dry nitrogen using Schlenk and glovebox techniques (Vacuum Atmospheres Omni-Lab) and using dry solvents (THF and toluene by passage through Vacuum Atmospheres solvent towers; pyridine was distilled from potassium and stored over molecular sieves; C_6D_6 was dried over potassium and trap-to-trap vacuum distilled). PhCN was pre-dried over $CaCO_3$, purified over activated alumina and distilled from P_2O_5, discarding the first and last 20 %, and was stored under nitrogen until required. ^{1}H NMR spectra were recorded at 298 K on a Bruker AVA400, or AVA600 spectrometer operating at 400.25 and 599.81 MHz respectively, and all spectra were referenced internally to residual solvent resonances; due to the paramagnetism of the compounds, no ^{13}C NMR spectra were recorded. The EPR spectra were recorded at 100 K on a Bruker EPX080 spectrometer by Dr Paul Murray at the University of Edinburgh. IR spectra were recorded as nujol mulls on a JASCO FT/IR 460 Plus spectrometer in the range 4000-400 cm^{-1}. The UV-Vis spectra were recorded on a Perkin Elmer Lambda 9 UV/Vis/NIR Spectrophotometer. Electrospray mass spectra were recorded using a Thermo LCQ instrument. Elemental analyses were carried out by Mr. Stephen Boyer at the London Metropolitan University.

Cyclic voltammograms were recorded under N_2 on 1.0 mM solutions of **1** in PhCN with $^nBu_4NBF_4$ (0.2 M) as the electrolyte. A conventional three-electrode cell was used made up of a working electrode of platinum wire embedded in glass, a silver wire reference electrode and a platinum foil counter electrode. Voltammograms were recorded at scan rates in the range 25 $mV.s^{-1}$ to 1.0 $V.s^{-1}$ using an Autolab PGstat12 potentiostat and the data were processed in GPES manager version 4.9. All voltammograms were referenced to the ferrocene/ferrocenium couple.

RRDE experiments were carried out in air-saturated 1.0 M aqueous CF_3CO_2H using a Pine Instruments RRD setup comprising a glassy carbon disk (area = 0.192 cm^2) and platinum ring, a Ag/AgCl chloride reference electrode separated from the bulk by a salt bridge, and a platinum wire counter electrode. The platinum ring was held at +1.0 V versus Ag/AgCl and the working electrode was rotated between 100 and 1000 rpm using a Pine Instruments AFMSRCE modulated speed rotator. Voltammograms were recorded at 50 $mV.s^{-1}$ using a PC-controlled AFCBB1 bipotentiostat. Before each experiment, the glassy carbon disk was cleaned with methanol, polished with 5 μm alumina, sonicated in distilled water, and rinsed with MeOH before drying in air. The disk was drop-coated with a freshly-made mM solution of [Co_2(L)] in dry THF. All the voltammograms are referenced to the Ag/AgCl reference electrode. The efficiency of the platinum ring was determined to be 23% by analysis of the ferri/ferrocycanide redox couple.

Solution catalytic oxygen reduction experiments were carried out using a modification of the procedures developed by Fukuzumi and Guilard.[10] Typically, solutions of [Co_2(L)] (1.0 mM), CF_3CO_2H (0.3 M), and ferrocene (0.3 M) were prepared under nitrogen. The [Co_2(L)] solution was freeze-pump-thaw degassed three times and placed under dry oxygen resulting in [O_2] = 8.5 mM. The catalytic medium was made up using these three solutions and diluting with oxygen or nitrogen-saturated PhCN to reach the reagent concentrations required. For example, 0.6 mL of the [Co_2(L)] solution, 1 mL of the ferrocene solution and 0.4 mL of nitrogen-saturated PhCN were placed in a UV-Vis quartz cell fitted with a septum-fitted air-tight screw cap. At t = 0 s, 1 mL of the CF_3CO_2H solution was added through the septum affording a 3 mL reaction mixture with reagent concentrations of [Co_2(L)] = 0.2 mM, [TFA] = 0.1 M, [Fc] = 0.1 M and [O_2] = 1.7 mM. The mixture was shaken to homogenize and the formation of ferrocenium was monitored over time at 620 nm (ε_{max} Fc^+ = 330 $M^{-1}.cm^{-1}$). In order to assess if any H_2O_2 had been formed, the catalytic reaction mixture was degassed at the end of the reaction and an aliquot (5 μL) diluted in nitrogen-saturated PhCN (3 mL), after which NaI (*ca*. 25 mg, large excess) was added and the quantity of I_3^- was determined by UV-vis spectrophotometry at λ_{max} = 365 nm (ε_{max} = 28000 $M^{-1}cm^{-1}$).

Synthesis of [Co_2(L)], 1: THF (5 mL) was added to a stirred mixture of H_4L (0.200 g, 0.23 mmol) and $LiN(SiMe_3)_2$ (0.156 g, 0.93 mmol, 4.1 eq) at −78 ºC and the mixture was allowed to warm to room temperature. After 4 h, the resulting solution was added dropwise to a suspension of $CoCl_2$ (0.060 g, 0.46 mmol, 2 eq) in THF (2 mL) at −78°C. The resulting mixture was allowed to warm to room temperature over 16 h during which a deep red solid formed. The reaction mixture was stored at − 20 °C for 24 h after which

the supernatant liquors were decanted and the solids dried under reduced pressure to yield 0.115 g, 51% of **1**. ^{1}H NMR (THF/C_6D_6, 599.81 MHz): δ_H 35.7 (s, 4H), 23.7 (s, 4H), 2.75 (s, 4H), -2.11 (s, 4H), -13.2 (s, 4H), -15.5 (br.s, 2H), -16.0 (s, 4H), -17.1 (s, 6H), -18.2 (s, 6H), -31.4 (s, 4H), -55.6 (vbr.s, 2H); IR (nujol): ν 1616 (w), 1580 (*C=N*), 1555 (*C=C*) cm^{-1}; UV-Vis (PhCN, N_2): λ_{max} 355 nm (ln ε=11.0), 430 (shoulder, 10.7); ESI-MS (THF-MeCN): *m/z* 974 ([M]$^+$, 20%, [Co_2(L)]), 991 ([M + 17]$^+$, 69%, [M]$^+$ + OH), 962 ([M + 17 - 29], 100%, [M]$^+$ + OH - Et), 945 ([M - 29]$^+$, 18%, [M]$^+$ - Et), 933 ([M + 17 - 58], 85%, [M]$^+$ + OH – 2Et), 916 ([M - 58]$^+$, <1%, [M]$^+$ - 2Et) ; Analysis. Found: C, 71.43; H, 5.03; N, 11.38. $C_{58}H_{48}N_8Co_2$ requires: C, 71.45; H, 4.96; N, 11.49 %; μ_{eff} (THF/C_6D_6) = 3.55 B.M; μ_{eff} (PhCN/TMS) = 1.69 B.M.

Reactions of 1 with O_2: 1 was dissolved in PhCN under N_2 in Teflon-tapped tubes/cells to form 1 mM solutions for NMR and EPR experiments or alternatively 20 μM solutions for UV-Vis experiments, freeze-pump-thaw degassed three times and exposed to oxygen.

^{1}H NMR (PhCN/C_6D_6 capillary, 400.25 MHz): Large regions are obscured by solvent signals in the aromatic region and aliphatic region, and accurate integration was prevented by the poor quality of the spectrum. The spectrum is mainly silent although a minor paramagnetic compound is observed at δ_H 20.5 (br.s), 10.1 (br.s), -2.79 (br.s), -5.09 (br.s), -6.59 (br.s), -7.63 (br.s), -8.08 (br.s), -11.4 (br.s); μ_{eff} (PhCN/TMS, triplicate) = 1.97 B.M.; EPR (X-band, PhCN, 100 K): g ~ 2.07, no resolved hyperfine; UV-Vis (PhCN): λ_{max} 358 nm (ln ε = 11.4), 449 (10.8).

Crystallographic details: X-Ray diffraction data on single crystals of [Co_2(L)][Co_2(*exo*-THF)$_2$(L)]·3PhMe (**1** and **1.THF**) were collected at 93 K on a Rigaku MM007 high brilliance RA generator equipped with Saturn 70 CCD detector using graphite monochromated using Mo Kα radiation (λ= 0.71073 Å) while the X-Ray diffraction data on the two sets of single crystals of [Co_2(*exo*-py)$_2$(L)]·4THF **1.py** and [$Co_2(H_3O_2)$(*exo*-py)$_2$(L)][BF_4]·1.8py **2** were collected at 100 K using an Oxford Cryosystems low temperature device attached to an Oxford Diffraction SuperNova dual wavelength diffractometer equipped with an Atlas CCD detector and operating in a mirror monochromated Cu*K*α radiation mode (λ = 1.54184 Å). Details of each data collection and refinement are given in Table S1. The structures were solved by direct methods or using SUPERFLIP[38] within the WinGX program suite[39] and refined by full-matrix least square refinement on $|F|^2$ using SHELXTL-97.[40] Except where stated below, all non-hydrogen atoms were refined with anisotropic displacement parameters and hydrogen atoms were placed at calculated positions and included as part of the riding model. The hydrogen atoms of the aqua hydroxy anion, H100 and H101, were located in the difference Fourier map using a 2-site free-variable refinement procedure and refined with fixed thermal parameters. In the structure of **1**/**1.THF**, some of the toluene solvent of crystallization was disordered and some carbon atoms (C3A3 and C3B3, C4A3 and C4B3, C4A2 and C4B2) were refined using an isotropic model. The structure of **2** presents a disordered pyridine solvent molecule on the 2-fold axis which was refined using an

isotropic model. In each unit cell, two BF_4 units could not be located and the structure exhibits large diameter channels along the *c* axis. The use of the SQUEEZE routine of PLATON[41] revealed voids located within the channels with a total solvent accessible volume of 1432.5 $Å^3$ and 422 electrons in the unit cell. This was attributed to two tetrafluoroborate anions (which require approximately 41 electrons each) and 8 diffuse pyridine molecules (which require approximately 42 electrons each) in the asymmetric unit. The refinement was much more stable after modeling with SQUEEZE.

Notes and references

[1] J. L. Dempsey, A. J. Esswein, D. R. Manke, J. Rosenthal, J. D. Soper and D. G. Nocera, *Inorg. Chem.*, 2005, **44**, 6879; M. Z. Jacobson, W. G. Colella and D. M. Golden, *Science*, 2005, **308**, 1901; M. Winter and R. J. Brodd, *Chem. Rev.*, 2004, **104**, 4245; M. Dresselhaus, G. Crabtree and M. Buchanan, *Basic Reserach Needs for the Hydrogen Economy*, U. S. Department of Energy, Washington DC, 2003; A. Boudghene Stambouli and E. Traversa, *Renew. Sustain. Energy Rev.*, 2002, **6**, 295; N. M. Marković, T. J. Schmidt, V. Stamenković and P. N. Ross, *Fuel Cells*, 2001, **1**, 105; B. C. H. Steele and A. Heinzel, *Nature*, 2001, **414**, 345.

[2] R. Borup, J. Meyers, B. Pivovar, Y. S. Kim, R. Mukundan, N. Garland, D. Myers, M. Wilson, F. Garzon, D. Wood, P. Zelenay, K. More, K. Stroh, T. Zawodzinski, J. Boncella, J. E. McGrath, M. Inaba, K. Miyatake, M. Hori, K. Ota, Z. Ogumi, S. Miyata, A. Nishikata, Z. Siroma, Y. Uchimoto, K. Yasuda, K.-i. Kimijima and N. Iwashita, *Chem. Rev.*, 2007, **107**, 3904.

[3] A. A. Gewirth and M. S. Thorum, *Inorg. Chem.*, 2010, **49**, 3557; K. Lee, L. Zhang and J. Zhang, in *PEM Fuel Cell Electrocatalysts and Catalyst Layers*, Springer London, 2008, pp. 715; D. A. Scherson, A. Palencsar, Y. Tolmachev and I. Stefan, *Adv. Electrochem. Sci. Eng.*, 2008, **10**, 191; F. C. Anson, C. Shi and B. Steiger, *Acc. Chem. Res*, 1997, **30**, 437.

[4] B. Wang, *J. Power Sources*, 2005, **152**, 1.

[5] R. Bashyam and P. Zelenay, *Nature*, 2006, **443**, 63.

[6] G. Wu, K. M. More, C. M. Johnston and P. Zelenay, *Science*, 2011, **332**, 443.

[7] M. Lefevre, E. Proietti, F. Jaouen and J. P. Dodelet, *Science*, 2009, **324**, 71 and references therein.

[8] J. P. Collman, A. Dey, Y. Yang, S. Ghosh and R. A. Decréau, *Proc. Nat. Acad. Sci.*, 2009, **106**, 10528; K. M. Kadish, L. Frémond, J. Shen, P. Chen, K. Ohkubo, S. Fukuzumi, M. E. Ojaimi, C. P. Gros, J.-M. Barbe and R. Guilard, *Inorg. Chem.*, 2009, **48**, 2571; K. M. Kadish, J. Shen, L. Frémond, P. Chen, M. El Ojaimi, M. Chkounda, C. P. Gros, J.-M. Barbe, K. Ohkubo, S. Fukuzumi and R. Guilard, *Inorg. Chem.* , 2008, **47**, 6726; S. Fukuzumi, *Chem. Lett.*, 2008, **37**, 808; P. D. Harvey, C. Stern, C. P. Gros and R. Guilard, *Coord. Chem. Rev.*, 2007, **251**, 401; J. D. Soper, S. V. Kryatov, E. V. Rybak-Akimova and D. G. Nocera, *J. Am. Chem. Soc.* , 2007, **129**, 5069; J. Rosenthal and D. G. Nocera, *Prog. Inorg. Chem.*, 2007, **55**, 483; K. M. Kadish, L. Frémond, F. Burdet, J.-M. Barbe, C. P. Gros and R. Guilard, *J. Inorg. Biochem.*, 2006, **100**, 858; K. M. Kadish, L. Frémond, Z. Ou, J. Shao, C. Shi, F. C. Anson, F. Burdet, C. P. Gros, J.-M. Barbe and R. Guilard, *J. Am. Chem. Soc.*, 2005, **127**, 5625; K. M. Kadish, J. Shao, Z. Ou, R. Zhan, F. Burdet, J.-M. Barbe, C. P. Gros and R. Guilard, *Inorg. Chem.*, 2005, **44**, 9023; J. P. Collman, M. Kaplun and R. A. Decréau, *Dalton Trans.*, 2006, 554; C. J. Chang, Z.-H. Loh, C. Shi, F. C. Anson and

D. G. Nocera, *J. Am. Chem. Soc.*, 2004, **126**, 10013; J. P. Collman, P. S. Wagenknecht and J. E. Hutchinson, *Angew. Chem. Int. Ed.*, 1994, **33**, 1537.

[9] J. Rosenthal and D. G. Nocera, *Acc. Chem. Res*, 2007, **40**, 543.

[10] S. Fukuzumi, K. Okamoto, C. P. Gros and R. Guilard, *J. Am. Chem. Soc.*, 2004, **126**, 10441.

[11] C. J. Chang, Y. Deng, C. Shi, C. K. Chang, F. C. Anson and D. G. Nocera, *Chem. Commun.*, 2000, 1355.

[12] Y. Le Mest, C. Inisan, A. Laouénan, M. L'Her, J. Talarmin, M. El Khalifa and J.-Y. Saillard, *J. Am. Chem. Soc.*, 1997, **119**, 6095.

[13] D. K. Dogutan, S. A. Stoian, R. McGuire, M. Schwalbe, T. S. Teets and D. G. Nocera, *J. Am. Chem. Soc.*, 2010, **133**, 131; R. McGuire Jr, D. K. Dogutan, T. S. Teets, J. Suntivich, Y. Shao-Horn and D. G. Nocera, *Chem. Sci.*, 2010, **1**, 411; J. Rosenthal, L. L. Chng, S. D. Fried and D. G. Nocera, *Chem. Commun.*, 2007, 2642; S. Y. Liu, J. D. Soper, J. Y. Yang, E. V. Rybak-Akimova and D. G. Nocera, *Inorg. Chem.*, 2006, **45**, 7572; J. P. Collman, R. Boulatov, C. J. Sunderland and L. Fu, *Chem. Rev.*, 2004, **104**, 561; C. J. Chang, L. L. Chng and D. G. Nocera, *J. Am. Chem. Soc.*, 2003, **125**, 1866.

[14] J. B. Love, *Chem. Commun.*, 2009, 3154 ; G. Givaja, M. Volpe, J. W. Leeland, M. A. Edwards, T. K. Young, S. B. Darby, S. D. Reid, A. J. Blake, C. Wilson, J. Wolowska, E. J. L. McInnes, M. Schröder and J. B. Love, *Chem. Eur. J.*, 2007, **13**, 3707; G. Givaja, A. J. Blake, C. Wilson, M. Schröder and J. B. Love, *Chem. Commun.*, 2003, 2508.

[15] J. L. Sessler, W.-S. Cho, S. P. Dudek, L. Hicks, V. M. Lynch and M. T. Huggins, *J. Porphyrins Phthalocyanines*, 2003, **7**, 97; J. M. Veauthier, E. Tomat, V. M. Lynch, J. L. Sessler, U. Mirsaidov and J. T. Markert, *Inorg. Chem.*, 2005, **44**, 6736; J. M. Veauthier, W.-S. Cho, V. M. Lynch and J. L. Sessler, *Inorg. Chem.*, 2004, **43**, 1220.

[16] G. Givaja, M. Volpe, M. A. Edwards, A. J. Blake, C. Wilson, M. Schröder and J. B. Love, *Angew. Chem. Int. Ed.*, 2007, **46**, 584.

[17] M. Volpe, H. Hartnett, J. W. Leeland, K. Wills, M. Ogunshun, B. Duncombe, C. Wilson, A. J. Blake, J. McMaster and J. B. Love, *Inorg. Chem.*, 2009, **48**, 5195.

[18] E. Askarizadeh, S. Bani Yaghoob, D. M. Boghaei, A. M. Z. Slawin and J. B. Love, *Chem. Commun.*, 2010, **46**, 710.

[19] E. Askarizadeh, A. M. J. Devoille, D. M. Boghaei, A. M. Z. Slawin and J. B. Love, *Inorg. Chem.*, 2009, **48**, 7491.

[20] F. Bolze, M. Drouin, P. D. Harvey, C. P. Gros, E. Espinosa and R. Guilard, *J. Porphyrins Phthalocyanines* 2003, **7**, 474.

[21] J. P. Collman, M. Marrocco, P. Denisevich, C. Koval and F. C. Anson, *J. Electroanal. Chem. Interfacial Electrochem.*, 1979, **101**, 117; J. P. Collman, P. Denisevich, Y. Konai, M. Marrocco, C. Koval and F. C. Anson, *J. Am. Chem. Soc.*, 1980, **102**, 6027; Y. Le Mest, M. L'Her, J. P. Collman, N. H. Hendricks and L. McElwee-White, *J. Am. Chem. Soc.*, 1986, **108**, 533.

[22] Y. Le Mest, M. L'Her, J. Courtot-Coupez, J. P. Collman, E. R. Evitt and C. S. Bencosme, *J. Chem. Soc., Chem. Commun.*, 1983, 1286.

[23] Y. Le Mest, C. Inisan, A. Laouenan, M. L'Her, J. Talarmin, M. El Khalifa and J.-Y. Saillard, *J. Am. Chem. Soc.*, 1997, **119**, 6095.

[24] C. K. Chang, *J. Chem. Soc., Chem. Commun.*, 1977, 800; J. P. Collman, P. Denisevich, Y. Konai, M. Marrocco, C. Koval and F. C. Anson, *J. Am. Chem. Soc.*, 1980, **102**, 6027; J. P. Collman, N. H. Hendricks, K. Kim and C. S. Bencosme, *J. Chem. Soc., Chem. Commun.*, 1987, 1537; J. P. Collman, J. E. Hutchison, M. Angel Lopez, A. Tabard, R. Guilard, W. K. Seok, J. A. Ibers and M. L'Her, *J. Am. Chem. Soc.*, 1992, **114**, 9869; L. M. Proniewicz, J. Odo, J. Goral, C. K. Chang and K. Nakamoto, *J. Am. Chem. Soc.*, 1989, **111**, 2105.

[25] J. P. Collman, J. E. Hutchison, M. A. Lopez, A. Tabard, R. Guilard, W. K. Seok, J. A. Ibers and M. L'Her, *J. Am. Chem. Soc.*, 1992, **114**, 9869.

[26] A. M. J. Devoille, P. Richardson, N. L. Bill, J. L. Sessler and J. B. Love, *Inorg. Chem.*, 2011, **50**, 3116.

[27] N. G. Connelly and W. E. Geiger, *Chem. Rev.*, 1996, **96**, 877.

[28] Y. Le Mest, M. L'Her and J. Y. Saillard, *Inorg. Chim. Acta*, 1996, **248**, 181.

[29] F. Allen, *Acta Crystallographr. Sect. B*, 2002, **58**, 380.

[30] A. Bino and D. Gibson, *J. Am. Chem. Soc.*, 1981, **103**, 6741; M. Ardon and A. Bino, *Inorg. Chem.*, 1985, **24**, 1343; M. Ardon and A. Bino, in *Solid State Chemistry*, Springer Berlin / Heidelberg, 1987, pp. 1; M. Ardon, A. Bino and W. G. Jackson, *Polyhedron*, 1987, **6**, 181.

[31] M. Ghiladi, J. T. Gomez, A. Hazell, P. Kofod, J. Lumtscher and C. J. McKenzie, *Dalton Trans.*, 2003, 1320.

[32] L. Brammer, *Dalton Trans.*, 2003, 3145.

[33] Z. Wang and S. M. Cohen, *Chem. Soc. Rev.*, 2009, **38**, 1315; J. Lee, O. K. Farha, J. Roberts, K. A. Scheidt, S. T. Nguyen and J. T. Hupp, *Chem. Soc. Rev.*, 2009, **38**, 1450.

[34] K. Oyaizu and E. Tsuchida, *J. Am. Chem. Soc.*, 2003, **125**, 5630.

[35] E. Kühn, V. Bulach and M. W. Hosseini, *Chem. Commun.*, 2008, 5104; M. Hoffmann, J. Kärnbratt, M. H. Chang, L. Herz, B. Albinsson and H. Anderson, *Angew. Chem. Int. Ed.*, 2008, **47**, 4993 and references therein; K. Fujisawa, A. Satake, S. Hirota and Y. Kobuke, *Chem. Eur. J.*, 2008, **14**, 10735; Y. Kuramochi, A. Satake and Y. Kobuke, *J. Am. Chem. Soc.*, 2004, **126**, 8668.

[36] J. W. Leeland, F. J. White and J. B. Love, *Chem. Commun.*, 2011, **47**, 4132.

[37] J. Rosenthal, PhD Thesis, Massachussetts Institute of Technology, 2007.

[38] L. Palatinus and G. Chapuis, *J. Appl. Cryst.*, 2007, **40**, 786.

[39] L. J. Farrugia, *J. Appl. Cryst.*, 1999, **32**, 837.

[40] G. M. Sheldrick, *Acta Cryst.*, 2008, **A64**, 112.

[41] A. L. Speck, Utrecht University, Utrecht, The Netherlands, 2001.